26. INFLUENCES OF NATURAL VARIABILITY AND ANTHROPOGENIC FORCING ON THE EXTREME 2015 ACCUMULATED CYCLONE ENERGY IN THE WESTERN NORTH PACIFIC

Wei Zhang, Gabriel A. Vecchi, Hiroyuki Murakami, Gabriele Villarini, Thomas L. Delworth, Karen Paffendorf, Rich Gudgel, Liwei Jia, Fanrong Zeng, and Xiaosong Yang

The extreme value of the 2015 western North Pacific (WNP) accumulated cyclone energy (ACE) was mainly caused by the sea surface warming in the eastern and central Pacific, with the anthropogenic forcing largely increasing the odds of the occurrence of this event.

Introduction. The 2015 tropical cyclone (TC) activity measured by the ACE [computed as the sum of the square of the maximum surface wind speed (MSW) over the TC duration when MSW is greater than 34 knots; e.g., Bell et al. 2000] was extremely high in the western North Pacific Ocean (Figs. 26.1a,b and 26.2a). The 2015 WNP ACE is the second highest since 1970 (with the highest being 1997) based on the Joint Typhoon Warning Center best track data for 1970–2014 and Unisys data for 2015 (http://weather.unisys.com/hurricane/), the highest since 1977 based on the Japan Meteorological Agency (JMA), and the highest since 1970 based on Shanghai Typhoon Institute (STI) data. Higher (lower) WNP ACE is generally observed during El Niño (La Niña) years, because TCs are formed more southeastward (northwestward) and stay longer (shorter) over the warm ocean surface (e.g., Camargo and Sobel 2005; Chan 2007). This shift in genesis and difference in tracks leads to a higher occurrence of the most intense typhoons, which is the main cause of a high ACE during El Niño years. An extremely strong El Niño event developed in 2015. While there has been major progress in the understanding of the El Niño–Southern Oscillation (ENSO)–WNP ACE association, the modulation of WNP ACE by anthropogenic forcing is still a challenging scientific question (e.g., Emanuel 2013; Lin and Chan 2015). Using observations and a suite of climate model experiments, this study attempts to assess whether and to what extent internal climate modes (e.g., ENSO) and anthropogenic forcing contributed to the extreme 2015 WNP ACE event.

Methodology. We use two coupled general circulation models (CGCMs): the Geophysical Fluid Dynamics Laboratory (GFDL) forecast-oriented low ocean resolution model (FLOR; Vecchi et al. 2014) and high-resolution FLOR (HiFLOR; Murakami et al. 2015a; Zhang et al. 2016b). TCs are identified and tracked using a tracking algorithm based on various model variables (Zhang et al. 2016a,b; see online Supplemental Material). The climatological values of WNP ACE in the observations, FLOR, and HiFLOR are different partly because of different spatial resolutions and climate mean states; we therefore analyze the WNP ACE values in terms of exceedance probabilities (e.g., 0.95, 0.99) of all the sampled ACE values in observations and simulations. Following Murakami et al. (2015b) and Yang et al. (2015), we use a probabilistic approach to examine the probability of a WNP ACE event as:

$$P(x) = \frac{\text{Number of years with ACE} \geq x}{\text{Total number of years}} \quad (1)$$

where x is a selected WNP ACE value and $P(x)$ represents the probability with WNP ACE larger than or equal to x. We use the fraction of attributable risk (FAR; e.g., Allen 2003; Stott et al. 2004) to quantify the FAR to human influence or anthropogenic forcing. FAR is defined as FAR = 1 – (P_0/P_1), where P_0 (P_1) is the probability of exceeding the observed TC

trend in the experiments without (with) anthropogenic forcing. We compute FAR using P_0 from a 1990 control experiment of FLOR and P_1 from a $2 \times CO_2$ experiment with the same model (van der Wiel et al. 2016). We also compute P_0 (P_1) from the two experiments of HiFLOR with radiative forcing representative of 1940 (2015; 1940 is also a strong El Niño year).

Natural Variability. The extremely high 2015 WNP ACE is mostly due to a large number of category 4 and 5 (C45; wind speed exceeding 58.1 m s^{-1}) TCs (Fig. 26.1a). There were 13 C45 TCs in the WNP during 2015, more than twice the climatological value of 6.3. The 2015 C45 proportion, defined by the number of C45 TCs divided by the basin-total TCs, is 0.48 while the climatology (1970–2015) is 0.25. The 2015 basin-total TC frequency (27) is slightly higher than climatology (25). The ENSO–WNP ACE association is supported by the high Niño-3.4 index in 2015, similar to those in 1987 and 1997 (Figs. 26.1b,c). The SST warming in 2015 extends westward to 160°E, and this provides favorable conditions for TC intensification because WNP TC intensification is influenced both by TC genesis location and ocean temperature (Wada and Chan 2008; Mei et al. 2015; Zhang et al. 2015). Previous studies suggested that factors such as the Pacific meridional mode (PMM), the Pacific decadal oscillation (PDO), and the Atlantic meridional mode (AMM) (see Supplemental Material) may also modulate WNP ACE (e.g., Chan 2008; Zhang et al. 2016a,c). The correlations between WNP ACE and the Niño-3.4 (significant at 0.01 level), PMM (significant at 0.01 level), and PDO (not significant at the 0.01 level) indices are positive, while the correlation between WNP
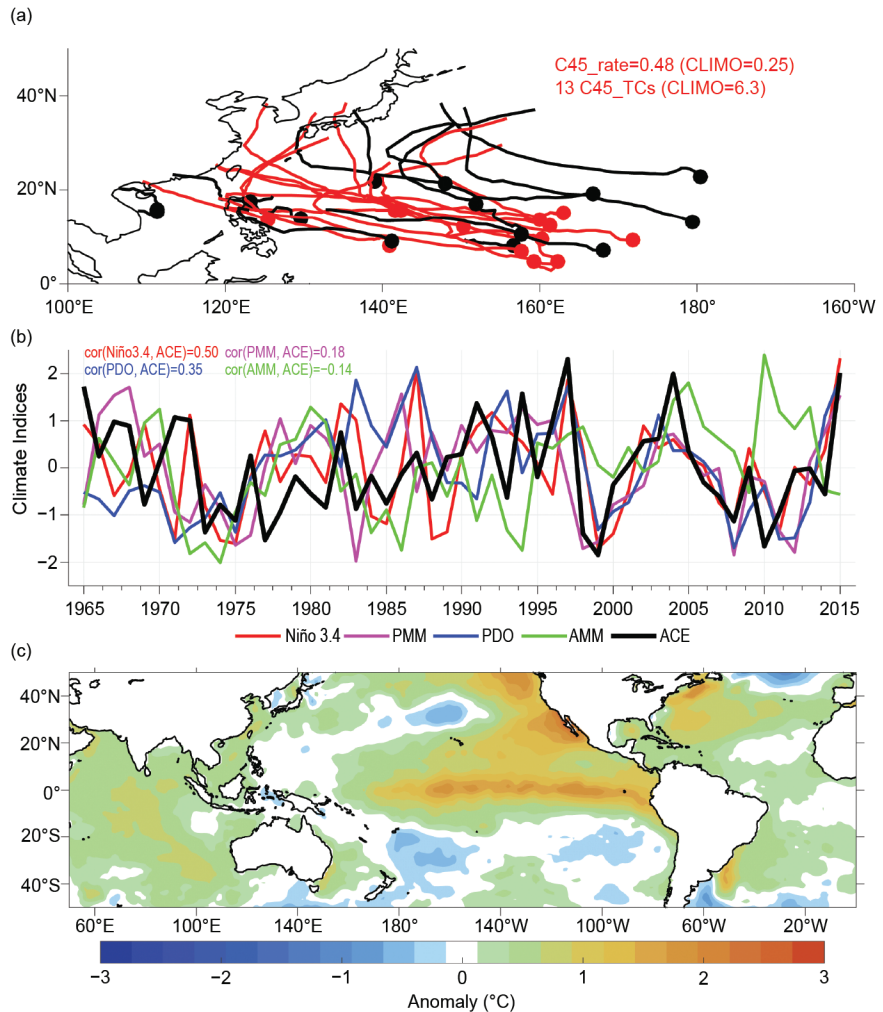

Fig. 26.1. (a) TC tracks in 2015 and C45 TCs (wind speed exceeding 58.1 m s^{-1}) are shown in red. The C45 proportion in 2015 is 0.48 while the climatology (1970–2015) is 0.26, with 13 (6.3) C45 TCs in 2015 (climatology; see Supplemental Material for data sources). **(b)** Time series of different annually averaged normalized climate indices (see legend) and ACE (black); Cor (Niño-3.4, ACE) denotes the correlation coefficient between Niño-3.4 index and WNP ACE for 1970–2015, while the others are defined likewise. **(c)** Sea surface temperature anomalies (°C) in 2015 computed with respect to the 1970–2000 base period.

ACE and the AMM is negative but not statistically significant (Fig. 26.1b, see Supplemental Material for more details of the indices). The Niño-3.4 and PMM indices in 2015 are strongly positive, contributing to the extreme 2015 WNP ACE. Therefore, internal climate modes, especially the strong El Niño, may have substantially contributed to the extreme 2015 WNP ACE by leading to an extremely high frequency of C45 TCs (Camargo and Sobel 2005).

Effect of Anthropogenic Forcing. We analyze two sets of experiments (i.e., 1990 control and $2 \times CO_2$ experiments) with FLOR. The probability density functions
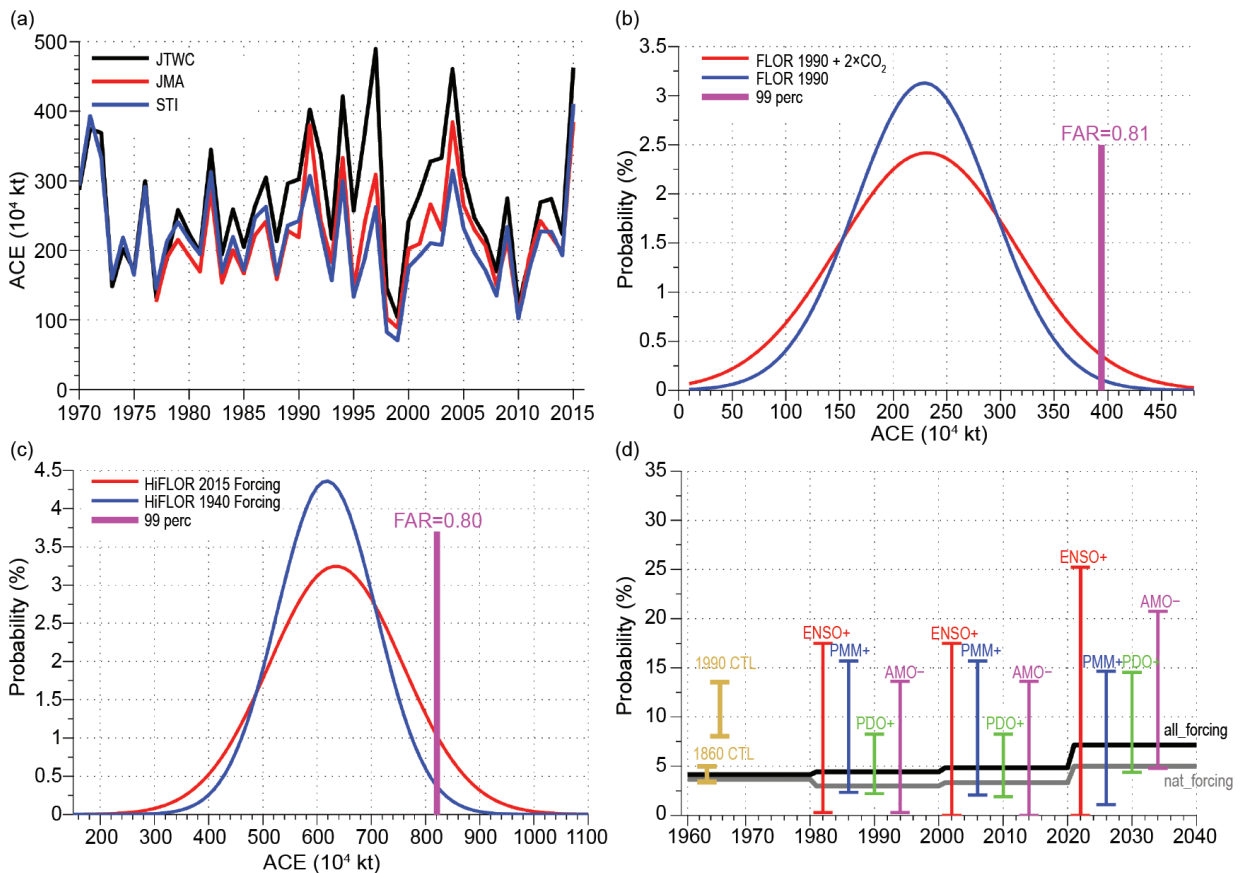
Fig. 26.2. (a) Annual WNP ACE based on observations. (b) PDFs of WNP ACE in 1990 (blue) and 2 × CO₂ (red) experiments with FLOR. (c) PDFs of WNP ACE in the experiments with radiative forcing representative of 1940 (blue) and 2015 (red) in HiFLOR. The magenta bars represent the 99th percentile of the ACE values (similar to observations) in FLOR/HiFLOR. (d) *P(x* = 95th percentile) in FLOR-FA all_forcing/nat_forcing multidecadal experiments with upper/lower limits of error bars represent ENSO+/− (red), PMM+/− (blue), PDO+/− (green), and AMO−/+ (magenta). The brown bars represent *P(x* = 95th percentile) in two control experiments with the widths representing the 0.95 confidence intervals. The black and gray curves represent *P(x* = 95th percentile) in samples of all_forcing and nat_forcing experiments, respectively.

(PDFs) of WNP ACE in FLOR 1990 control and 2 × CO₂ experiments have similar mean values while their variances are different, with a fatter tail in the 2 × CO₂ experiment (Fig. 26.2b). We select the ACE values in the 99th percentile of FLOR 1990 to calculate FAR, consistent with the percentile of the observed 2015 WNP ACE (Figs. 26.2a,b). The FAR in the 1990 control and 2 × CO₂ experiments of FLOR are 0.81, indicating that anthropogenic forcing can substantially increase the risk of having extreme WNP ACE events higher than or equal to the 2015 event. To further substantiate this finding, we also analyze P_0 and P_1 in the two experiments of HiFLOR with radiative forcing representative of 1940 and 2015. The PDFs of WNP ACE in HiFLOR also have a fatter tail in the experiment with radiative forcing representative of 2015 compared with that of 1940 (Fig. 26.2c). The FAR

in HiFLOR is 0.80, close to 0.81 in the experiments with FLOR (Figs. 26.2b,c).

We ran 35-member simulations with all forcing (natural and anthropogenic under RCP 4.5 scenario) and 30-member multidecadal simulations with natural forcing from 1961 to 2040 (see Supplemental Material). For each 20-year period from 1961, 1300 (20 × 35 + 20 × 30) samples (years) were available to calculate *P(x)*. We define a simulated positive (or negative) phase of ENSO, PDO, PMM, and AMO as these indices exceeding (falling below) one (minus one) standard deviation and estimate the amplitude of *P(x)* between the two phases. Figure 26.2d illustrates the results for *P(x* = 95th percentile). *P(x* = 95th percentile) in all_forcing experiments increases from 1960 to 2040, suggesting that the external forcing tends to increase the odds of occurrence of extreme

WNP ACE. There is a sharp increase in $P(x = 95th$ percentile) during 2020–40 (Fig. 26.2d). In addition, the $P(x = 95th$ percentile) in nat_forcing experiments also largely increases in 1960–2060, except for a slight decrease from 1960–80 to 1980–2000. The $P(x = 95th$ percentile) in all_forcing experiments are higher than those in nat_forcing experiments, indicating that anthropogenic forcing increases the risk of having extreme WNP ACE events. The results based on FLOR-FA 1860 and 1990 control experiments are also shown in the left of Fig. 26.2d, providing additional support to these conclusions. For each 20-year subperiod in 1980–2040, ENSO produces the largest variability of WNP ACE (Fig. 26.2d). The variability associated with ENSO is larger than that associated with radiative forcing (Fig. 26.2d). Therefore, the extreme 2015 WNP ACE may be mainly modulated by natural climate modes, especially by the strong El Niño, with the anthropogenic forcing increasing the risk of 2015 having a season with an extremely high WNP ACE. This risk is predicted to continue to increase in the next few decades, increasing the probability of having seasons with a WNP ACE equal to or higher than 2015 in the future.

Discussions and Conclusions. We have observed an extremely active TC season in the WNP in 2015, with an extremely high ACE and frequency of C45 TCs. The 2015 season may be caused mainly by warm ocean surface temperatures in the tropical Pacific, characterized by a strong El Niño event, with other climate modes (e.g., PMM) potentially playing a role. We have found that anthropogenic forcing has substantially increased the risk of having WNP ACE higher than or equal to such an extreme event. Although the changes in WNP ACE under anthropogenic forcing are still unclear (e.g., Emanuel 2013; Lin and Chan 2015), both GFDL FLOR and HiFLOR do suggest that the annual WNP ACE tends to become more extreme because of anthropogenic forcing. The two models also suggest that the variability of WNP ACE attributable to climate modes will increase at a much higher rate than as a result of anthropogenic forcing. The frequency of strong El Niño events is projected to increase due to greenhouse warming (Cai et al. 2014), which in turn could potentially lead to a higher frequency of WNP seasons with high values of ACE.

REFERENCES

Allen, M., 2003: Liability for climate change. *Nature*, **421**, 891–892.

Bell, G. D., and Coauthors, 2000: Climate assessment for 1999. *Bull. Amer. Meteor. Soc.*, **81 (6)**, S1–S50.

Cai, W., and Coauthors, 2014: Increasing frequency of extreme El Niño events due to greenhouse warming. *Nat. Climate Change*, **4**, 111–116, doi:10.1038/nclimate2100.

Camargo, S. J., and A. H. Sobel, 2005: Western North Pacific tropical cyclone intensity and ENSO. *J. Climate*, **18**, 2996–3006.

Chan, J. C. L., 2007: Interannual variations of intense typhoon activity. *Tellus*, **59A**, 455–460.

——, 2008: Decadal variations of intense typhoon occurrence in the western North Pacific. *Proc. Roy. Soc. London*, **464A**, 249–272.

Emanuel, K. A., 2013: Downscaling CMIP5 climate models shows increased tropical cyclone activity over the 21st century. *Proc. Natl. Acad. Sci. USA*, **110**, 12219–12224, doi:10.1073/pnas.1301293110.

Lin, I. I., and J. C. L. Chan, 2015: Recent decrease in typhoon destructive potential and global warming implications. *Nat. Commun.*, **6**, 7182, doi:10.1038/ncomms8182.

Mei, W., S.-P. Xie, F. Primeau, J. C. McWilliams, and C. Pasquero, 2015: Northwestern Pacific typhoon intensity controlled by changes in ocean temperatures. *Sci. Adv.*, **1**, e1500014, doi:10.1126/sciadv.1500014.

Murakami, H., and Coauthors, 2015a: Simulation and prediction of category 4 and 5 hurricanes in the high-resolution GFDL HiFLOR coupled climate model. *J. Climate*, **28**, 9058–9079. 10.1175/JCLI-D-15-0216.1.

——, G. A. Vecchi, T. L. Delworth, K. Paffendorf, L. Jia, R. Gudgel, and F. Zeng, 2015b: Investigating the influence of anthropogenic forcing and natural variability on the 2014 Hawaiian hurricane season [in "Explaining Extreme Events of 2014 from a Climate Perspective"]. *Bull. Amer. Meteor. Soc.*, **96 (12)**, S115–S119, doi:10.1175/BAMS-D-15-00119.1.

Stott, P. A., D. A. Stone, and M. R. Allen, 2004: Human contribution to the European heatwave of 2003. *Nature*, **432**, 610–614, doi:10.1038/nature03089.

Van der Wiel, K., and Coauthors, 2016: The resolution dependence of contiguous US precipitation extremes in response to CO_2 forcing. *J. Climate*, **29**, 7991–8012, doi:10.1175/JCLI-D-16-0307.1.

Vecchi, G. A., and Coauthors, 2014: On the seasonal forecasting of regional tropical cyclone activity. *J. Climate*, **27**, 7994–8016, doi:10.1175/JCLI-D-14-00158.1.

Wada, A., and J. C. L. Chan, 2008: Relationship between typhoon activity and upper ocean heat content. *Geophys. Res. Lett.*, **35**, L17603, doi:10.1029/2008GL035129.

Yang, X., G. A. Vecchi, T. L. Delworth, K. Paffendorf, R. Gudgel, L. Jia, S. D. Underwood, and F. Zeng, 2015: Extreme North America winter storm season of 2013/14: Roles of radiative forcing and the global warming hiatus [in "Explaining Extreme Events of 2014 from a Climate Perspective"]. *Bull. Amer. Meteor. Soc.*, **96 (12)**, S25–S28, doi:10.1175/BAMS-D-15-00133.1.

Zhang, W., Y. Leung, and K. Fraedrich, 2015: Different El Niño types and intense typhoons in the western North Pacific. *Climate Dyn.*, **44**, 2965–2977, doi:10.1007/s00382-014-2446-4.

——, and Coauthors, 2016a: The Pacific meridional mode and the occurrence of tropical cyclones in the western North Pacific. *J. Climate*, **29**, 381–398, doi:10.1175/JCLI-D-15-0282.1.

——, and Coauthors, 2016b: Improved simulation of tropical cyclone responses to ENSO in the western North Pacific in the high-resolution GFDL HiFLOR coupled climate model. *J. Climate*, **29**, 1391–1415, doi:10.1175/JCLI-D-15-0475.1.

——, G. A. Vecchi, G. Villarini, H. Murakami, A. Rosati, X. Yang, L. Jia, and F. Zengand, 2016c: Modulation of western North Pacific tropical cyclone activity by the Atlantic meridional mode. *Climate Dyn.*, in press, doi:10.1007/s00382-016-3099-2.